

Robust Chaos and the Continuity of Attractors.

P.A. Glendinning[†] and D.J.W. Simpson[‡]

[†]School of Mathematics, University of Manchester, Oxford Road, Manchester, M13 9PL, UK.

[‡]School of Fundamental Sciences, Massey University, Palmerston North, New Zealand

July 1, 2019

Abstract

As the parameters of a map are varied an attractor may vary continuously in the Hausdorff metric. The purpose of this paper is to explore the continuation of chaotic attractors. We argue that this is not a helpful concept for smooth unimodal maps for which periodic windows fill parameter space densely, but that for piecewise-smooth maps it provides a way to delineate structure within parameter regions of robust chaos and form a stronger notion of robustness. We obtain conditions for the continuity of an attractor and demonstrate the results with coupled skew tent maps, the Lozi map, and the border-collision normal form.

1 Introduction

Let f_μ be a family of maps on \mathbb{R}^p that vary continuously with respect to a parameter $\mu \in M \subset \mathbb{R}^q$, where M is compact with non-empty interior. We say that f_μ exhibits *robust chaos* in M if f_μ has a chaotic attractor for each $\mu \in M$ and there exist $\mu_1, \mu_2 \in M$ such that f_{μ_1} is not topologically conjugate to f_{μ_2} [1, 2]. This last stipulation prohibits the trivial case that f_μ undergoes no topological change as μ is varied. While robust chaos does not occur for generic smooth maps of the interval [3], it appears to be typical for maps that are piecewise-smooth [4].

In applications that utilise chaos, such as mixing [5], spacecraft trajectories [6], and encryption [7], robust chaos is often a desired property. It seems reasonable that chaotic attractors at nearby parameter values should be in some way related because the map varies continuously even if the details of the dynamics can change. The aim of this paper is to give mathematical meaning to this sense of sameness by using continuity in the Hausdorff metric. We show how this adds structure to parameter regimes of robust chaos, and in fact a layered structure when multiple attractors coexist.

The continuity of attractors in the Hausdorff metric has been useful in a number of problems. Stuart and Humphries [8] use it with the semi-distance (see §2) to assess the numerical approximation of dynamical systems via the geometry of attractors rather than their dynamics. This is a natural extension to continuation techniques for periodic orbits.

There are also fairly general results for the continuity of global attractors of semi-flows [9]. In particular Hoang *et. al.* [10] develop a concise and effective characterisation of the continuity of global attractors and we follow their approach in §5.

Outside of §5 we investigate the continuity of attractors through a series of examples. Our motivation is to develop ideas which can be used easily. This, together with the fact that our definition of attractors (see §2) is local, means we need a slightly more complicated continuity argument than that of [10], although the underlying principles are the same.

2 Definitions

Let d be a metric on \mathbb{R}^p . The (asymmetric) *semi-distance* between sets $X, Y \subseteq \mathbb{R}^p$ is defined as

$$d_a(X, Y) = \sup_{x \in X} \inf_{y \in Y} d(x, y), \quad (1)$$

see Fig. 1 for a visualisation. The Hausdorff distance is the following symmetric version of this semi-distance:

$$d_H(X, Y) = \max[d_a(X, Y), d_a(Y, X)]. \quad (2)$$

We also write

$$B_r(X) = \{y \in \mathbb{R}^p \mid d_a(y, X) \leq r\},$$

to denote the closed ball of radius $r > 0$ around a set $X \subseteq \mathbb{R}^p$.

Definition 2.1. Let f be a continuous map on \mathbb{R}^p . A compact set $\mathcal{A} \subset \mathbb{R}^p$ is an *attractor* of f if

- i) $f(\mathcal{A}) = \mathcal{A}$,
- ii) \mathcal{A} contains a dense orbit, and
- iii) there exists $r > 0$ such that $d_a(f^n(x), \mathcal{A}) \rightarrow 0$ as $n \rightarrow \infty$ for all $x \in B_r(\mathcal{A})$.

If in addition Lyapunov exponents of typical points are positive then we say \mathcal{A} is a *chaotic* attractor.

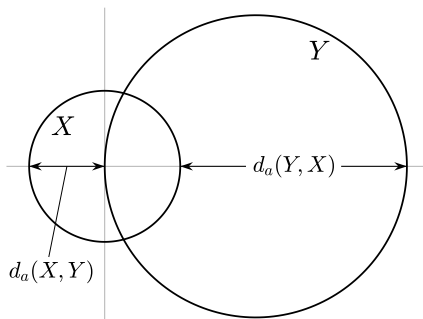


Figure 1: The semi-distance (1) for two closed discs in \mathbb{R}^2 .

Now suppose a family of maps f_μ has an attractor \mathcal{A}_μ for all $\mu \in M$. To say that \mathcal{A}_μ is continuous in the Hausdorff metric at some $\mu \in M$ means the following: for all $\varepsilon > 0$ there exists $\delta > 0$ such that $d_H(\mathcal{A}_\mu, \mathcal{A}_\nu) < \varepsilon$ whenever $\nu \in M$ and $|\mu - \nu| < \delta$.

3 Tent maps

Here we consider the tent map

$$T_s(x) = \begin{cases} sx, & 0 \leq x \leq \frac{1}{2}, \\ s(1-x), & \frac{1}{2} \leq x \leq 1. \end{cases} \quad (3)$$

If $1 < s \leq 2$ the tent map has a unique attractor on $[0, 1]$, see Fig. 2. If $\sqrt{2} \leq s \leq 2$, the attractor is the interval $I_0(s) = [s(1 - \frac{s}{2}), \frac{s}{2}]$. Otherwise it is the union of 2^n disjoint closed intervals where $\sqrt{2} \leq s^{2^{n-1}} < 2$, see [11, 12]. Lemma 3.1 below shows that, despite having different numbers of connected components, the attractor is continuous in the Hausdorff metric. In a similar way stable periodic solutions in period-doubling cascades are continuous because, despite a change in the period at period-doubling bifurcations, the attractor does not experience a jump in phase space. In this and the next section we use $d(x, y) = |x - y|$.

Lemma 3.1. *The attractor of the tent map (3) is continuous for $1 < s \leq 2$.*

Proof. If $\sqrt{2} < s \leq 2$ the attractor is $I_0 = [T_s^2(\frac{1}{2}), T_s(\frac{1}{2})]$ which is continuous since its endpoints vary continuously.

Next we verify continuity at $s = \sqrt{2}$. As $s \rightarrow \sqrt{2}$ from above the attractor is $I_0(s)$ and simply converges to $I_0(\sqrt{2})$. As $s \rightarrow \sqrt{2}$ from below the attractor is the disjoint union $I_1(s) \cup I_2(s)$ where

$$I_1(s) = [T_s^2(\frac{1}{2}), T_s^4(\frac{1}{2})], \quad I_2(s) = [T_s^3(\frac{1}{2}), T_s(\frac{1}{2})],$$

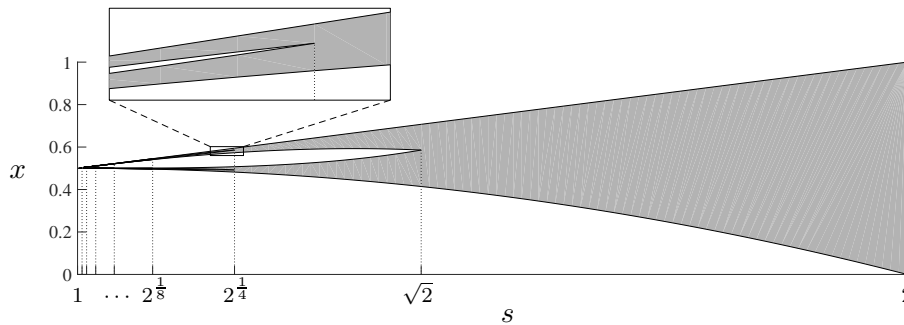


Figure 2: The attractor of the tent map (3) for different values of the parameter s . As the value of s is decreased the number of intervals that comprise the attractor doubles at $s = 2^{\frac{1}{2^n}}$ for each $n \geq 1$. These band-splittings do not produce a jump in the Hausdorff distance, Lemma 3.1.

see Fig. 3. The lower endpoint of $I_1(s)$ and the upper endpoint of $I_2(s)$ converge to the endpoints of $I_0(\sqrt{2})$, so it remains to show that the size of the gap between $I_1(s)$ and $I_2(s)$ converges to zero as $s \rightarrow \sqrt{2}$. Indeed a direct calculation produces

$$T_s^3\left(\frac{1}{2}\right) - T_s^4\left(\frac{1}{2}\right) = s(s-1)\left(1 - \frac{s^2}{2}\right),$$

which vanishes at $s = \sqrt{2}$. This shows that $d_H(I_0(\sqrt{2}), I_1(s) \cup I_2(s)) \rightarrow 0$ as $s \rightarrow \sqrt{2}$ from below, so the attractor of (3) is continuous at $s = \sqrt{2}$.

If $s < \sqrt{2}$ then T_s^2 restricted to $I_1(s)$ or $I_2(s)$ is a linear rescaling of T_{s^2} restricted to $I_0(s^2)$ and so the proof can be completed by considering higher iterates in an inductive fashion [11, 12]. \square

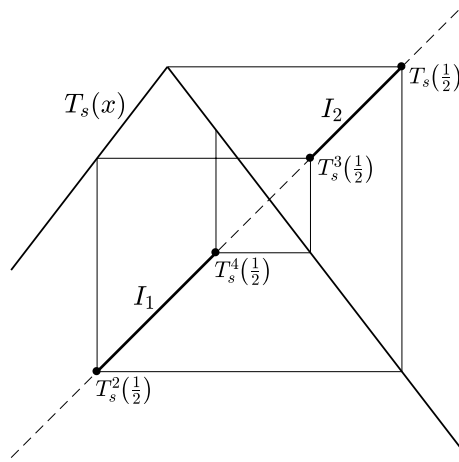


Figure 3: A cobweb diagram showing the two-band attractor of the tent map (3) for $2^{\frac{1}{4}} < s < \sqrt{2}$.

4 Quadratic maps

The aim of this section is to argue that the continuation of chaotic attractors is not helpful for smooth maps (at least in one dimension). To do this we rely on a number of standard results for quadratic families which can be found, for example, in [3, 13]. Smooth families of unimodal maps f_μ with a single maximum occurring at c (the critical point) can be described in terms of symbolic dynamics. Every orbit defines a sequence of C 's, L 's and R 's by seeing if the n^{th} point of the orbit equals c , lies to the left of c , or lies to the right of c , respectively. There is a natural order on these sequences: if W is a finite sequence of symbols (a word) then $WL < WC < WR$ if W has an even number of R 's and the inequality is reversed if W has an odd number of R 's (this is connected with the fact that f^n is decreasing if there are an odd number of R 's). The *kneading invariant* of f_μ is the symbol sequence K_μ associated with $f_\mu(c)$. There are consistency conditions on the possible sequences that can occur: if the

critical point is not periodic then this condition is simply that K_μ is the maximal element of its shifts:

$$\sigma^k(K_\mu) \leq K_\mu, \quad \text{for all } k \geq 1, \quad (4)$$

where σ is the shift map. Families which depend smoothly (C^1) on the parameter are full if all possible consistent kneading invariants between those of the end-points do actually occur in the family. A family is monotonic if the kneading invariant is monotonic in the parameter (this means in particular that certain behaviour is not repeated). The standard quadratic maps are full and monotonic. Further conditions such as convexity or negative Schwarzian derivative imply that there is a unique attractor at every parameter value. Recall that f_μ is in a period- n window if there exists $n > 0$ and an interval J such that f_μ^n restricted to J is a unimodal map.

Lemma 4.1. *Suppose that f_μ is a smooth unimodal map (at least C^2 in phase space and C^1 in the parameter) and has a unique attractor at each parameter value μ in some closed interval I . If there is a parameter $\mu_0 \in \text{int}(I)$ with a non-degenerate saddle-node bifurcation of period $k > 1$, then the attractor is not continuous in the Hausdorff metric at μ_0 .*

Proof. We may assume without loss of generality that f_{μ_0} is not in a period r window, $r < k$ (otherwise consider f^r). In particular we can assume that the parameter lies in the single band region (the equivalent of $s > \sqrt{2}$ in the tent map) with kneading invariant greater than RLR^∞ . The kneading invariant at μ_0 is $K(\mu_0) = (WC)^\infty$ with W a sequence of L 's and R 's starting RL . Choose the sign of μ so that the periodic orbit created by the saddle-node bifurcation exists if $\mu > \mu_0$. If $\mu < \mu_0$ with $|\mu - \mu_0|$ small, then the kneading invariant starts $(WE)^n \dots$, with $n \rightarrow \infty$ as $\mu \rightarrow \mu_0$ from below and

$$E = \begin{cases} L, & \text{W has an even number of } R\text{'s,} \\ R, & \text{W has an odd number of } R\text{'s.} \end{cases}$$

It is now an elementary exercise to show that the sequences $(WE)^n WLR^\infty$ if $E = L$ or $(WE)^n WR^\infty$ if $E = R$ satisfy the consistency conditions (4), and since the points c and its images define a Markov partition (they are Misiurewicz points) and are not in a period r window the attractor is the interval $I_{\mu_n} = [f_{\mu_n}^2(c), f_{\mu_n}(c)]$. Thus arbitrarily close to the bifurcation value μ_0 the attractor is an interval.

If $\mu = \mu_0$ then there is a non-hyperbolic periodic orbit W_k of period k which is the attractor for f and k non-trivial close intervals B_i , $i = 1, \dots, k$, which are the immediate basins of attraction of the periodic orbit of period k (one end point of each of these intervals is a point of period k ; these are one-sided basins of attraction).

We have already seen that in any small neighbourhood of μ_0 there exists μ such that the attractor of f_μ is an interval I_{μ_n} , and there exists i such that $B_i \subset I_{\mu_n}$ (as the period $k \geq 3$). Hence if $|B_i| = 2\varepsilon$, $d_a(I_{\mu_n}, W_k) > \varepsilon$ since the closest that W_k can be to the part of the attractor inside B_i is ε . Hence the attractor is not continuous at μ_0 . \square

Corollary 4.2. *The only non-trivial intervals on which the attractor of the logistic map is continuous in the Hausdorff metric are the period-doubling cascades of stable periodic orbits.*

Proof. Between any two topologically distinct chaotic attractors there exist parameter values with saddle-node bifurcations of periodic orbits. \square

5 Uniform continuity and continuation

In this section we derive general results for the continuity of attractors. Our approach follows Hoang *et. al.* [10] with some technical additions required to accommodate local attractors that will be useful when we come to the Lozi map in §7.

Let f_μ be a family of maps on \mathbb{R}^p where $\mu \in M$ and $M \subset \mathbb{R}^q$ is compact. Assume f_μ varies continuously in phase space and in μ . Assume that for each $\mu \in M$, the map f_μ has an attractor \mathcal{A}_μ and let $r_\mu > 0$ be a suitable value for part (iii) of Definition 2.1. Two further assumptions are needed.

(A1) There exists compact $\Omega \subset \mathbb{R}^p$ such that $B_{r_\mu}(\mathcal{A}_\mu) \subseteq \Omega$ for all $\mu \in M$.

(A2) For all $\mu \in M$ there exists compact $N_\mu \subseteq \Omega$, continuous (with respect to μ) in the Hausdorff metric, such that $f(N_\mu) \subseteq N_\mu$ and $\mathcal{A}_\mu = \text{cl}(\cap_{n=0}^\infty f_\mu^n(N_\mu))$.

These are the natural generalizations of (L2) and (L3) of [10]. The following lemma shows that at each stage of the construction of the attractor by iterates of N_μ , the sets remain close (this is equivalent to Lemma 3.1 of [10]).

Lemma 5.1. *Suppose f_μ is continuous with an attractor \mathcal{A}_μ and (A1) and (A2) hold. For each $n \geq 0$, $f_\mu^n(N_\mu)$ is continuous in the Hausdorff metric in M .*

Proof. Choose any $n \geq 0$ and $\varepsilon > 0$. Since f^n is continuous in x and μ and Ω and M are compact, by the Heine-Cantor theorem f^n is uniformly continuous in x and μ . Thus there exist $\delta_\Omega, \delta_M > 0$ such that for all $x, y \in \Omega$ with $d(x, y) < \delta_\Omega$ and all $\mu, \nu \in M$ with $|\mu - \nu| < \delta_M$ we have $d(f_\mu^n(x), f_\nu^n(y)) < \varepsilon$.

Since N_μ is continuous on the compact set M it is similarly uniformly continuous and so there exists $\delta_1 > 0$ such that for all $\mu, \nu \in M$ with $|\mu - \nu| < \delta_1$ we have $d_H(N_\mu, N_\nu) < \delta_\Omega$.

Let $\delta = \min(\delta_1, \delta_M)$. Choose any $\mu, \nu \in M$ with $|\mu - \nu| < \delta$. Then

$$d_a(f_\mu^n(N_\mu), f_\nu^n(N_\nu)) = \sup_{x \in N_\mu} \inf_{y \in N_\nu} d(f_\mu^n(x), f_\nu^n(y)) < \varepsilon,$$

because for all $x \in N_\mu$ there exists $y \in N_\nu$ such that $d(x, y) < \delta_\Omega$. We similarly have $d_a(f_\nu^n(N_\nu), f_\mu^n(N_\mu)) < \varepsilon$, thus $d_H(f_\mu^n(N_\mu), f_\nu^n(N_\nu)) < \varepsilon$, as required. \square

Theorem 5.2. *If the conditions of Lemma 5.1 hold and $d_H(f_\mu^n(N_\mu), \mathcal{A}_\mu) \rightarrow 0$ as $n \rightarrow \infty$ uniformly in M , then \mathcal{A}_μ is continuous in the Hausdorff metric in M .*

Proof. Choose any $\varepsilon > 0$. There exists $n_0 \geq 0$ such that for all $\mu \in M$ and all $n \geq n_0$ we have $d_H(f_\mu^n(N_\mu), \mathcal{A}_\mu) < \frac{\varepsilon}{3}$. By Lemma 5.1, $f_\mu^n(N_\mu)$ is continuous in M , but M is compact so the continuity is uniform, thus there exists $\delta > 0$ such that for all $\mu, \nu \in M$ with $|\mu - \nu| < \delta$ we have $d_H(f_\mu^n(N_\mu), f_\nu^n(N_\nu)) < \frac{\varepsilon}{3}$. Then for any $\mu, \nu \in M$ with $|\mu - \nu| < \delta$ we have

$$d_H(\mathcal{A}_\mu, \mathcal{A}_\nu) \leq d_H(\mathcal{A}_\mu, f_\mu^n(N_\mu)) + d_H(f_\mu^n(N_\mu), f_\nu^n(N_\nu)) + d_H(f_\nu^n(N_\nu), \mathcal{A}_\nu) < \varepsilon.$$

\square

The most remarkable aspect of Hoang *et. al.* [10] is their proof that uniform convergence to the attractor with respect to the parameter implies continuity of the attractor, and, if the convergence is only pointwise then the continuity at least occurs on a residual set. Recall, a *residual set* is the complement of a countable union of nowhere dense sets, and every residual set is dense. The uniform case is covered above by Theorem 5.2, so it remains for us to address pointwise convergence. The following technical result will be needed, and indeed, contains all the hard work!

Lemma 5.3 (Hoang *et. al.* [10]). *Let \mathcal{X} be a complete metric space, \mathcal{Y} be a metric space, and $g_n : \mathcal{X} \rightarrow \mathcal{Y}$ be a family of continuous maps. If the pointwise limit $g(x) = \lim_{n \rightarrow \infty} g_n(x)$ exists for each $x \in \mathcal{X}$, then g is continuous on a residual subset of \mathcal{X} .*

In our case, \mathcal{X} is the parameter space M and \mathcal{Y} the space of compact subsets of \mathbb{R}^p with the Hausdorff metric.

Theorem 5.4. *Suppose f_μ is continuous with an attractor \mathcal{A}_μ and (A1) and (A2) hold. Then \mathcal{A}_μ is continuous in the Hausdorff metric on a residual subset of M .*

Proof. Let $g_n(\mu) = f_\mu^n(N_\mu)$ and $g(\mu) = \mathcal{A}_\mu$. By Lemma 5.1, each $g_n(\mu)$ is continuous, and by (A2), $g_n(\mu) \rightarrow g(\mu)$ as $n \rightarrow \infty$ for each $\mu \in M$, so the result follows by Lemma 5.3. \square

6 Coupled skew tent maps

In the next three sections we identify continuous chaotic attractors in three different piecewise-linear maps. In these sections d is the Euclidean metric on \mathbb{R}^2 .

Skew tent maps generalise (3) to allow two slopes that differ in absolute value. Specifically we consider

$$\tilde{T}_s(z) = \begin{cases} sz, & 0 \leq z \leq \frac{1}{s}, \\ \frac{s}{s-1}(1-z), & \frac{1}{s} \leq z \leq 1, \end{cases} \quad (5)$$

where $1 < s < 2$. Each \tilde{T}_s , see Fig. 4, is a skew tent map on $[0, 1]$ equivalent to a full shift on two symbols. As considered originally in [14], here we use (5) to form the coupled skew

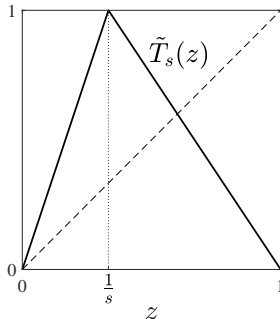


Figure 4: The skew tent map (5).

tent map

$$f_{s,\omega}(x) = \begin{bmatrix} (1-\omega)\tilde{T}_s(x_1) + \omega\tilde{T}_s(x_2) \\ \omega\tilde{T}_s(x_1) + (1-\omega)\tilde{T}_s(x_2) \end{bmatrix}, \quad (6)$$

where $0 \leq \omega \leq \frac{1}{2}$ is a measure of the coupling strength. This is a map on $[0, 1] \times [0, 1]$ and we write $x = (x_1, x_2) \in \mathbb{R}^2$.

The diagonal $x_1 = x_2$ is an invariant set that is stable for sufficiently large values of ω . As the value of ω is decreased a ‘blowout bifurcation’ occurs when typical transverse Lyapunov exponents become positive at $\omega = \frac{1}{2}(1 - e^{-\gamma})$, where $\gamma = \ln(s) - (1 - \frac{1}{s})\ln(1 - s)$, see [15]. However, some orbits on the diagonal become transversely unstable before the blowout bifurcation. This first occurs at $\omega = \frac{1}{2s}$ and is responsible for the creation of a two-dimensional attractor.

Theorem 6.1 (Glendinning [15]). *Let $\frac{\sqrt{5}+1}{2} < s < 2$. Let \mathcal{D} be the closed quadrilateral $ORIR'$ where*

$$O = (0, 0), \quad R = \left(2\omega, \frac{1-2\omega+2\omega^2}{1-\omega}\right), \quad I = (1, 1), \quad R' = \left(\frac{1-2\omega+2\omega^2}{1-\omega}, 2\omega\right),$$

see Fig. 5. If $0 < \omega < \frac{1}{2s}$ then \mathcal{D} is the unique attractor of (6), whilst if $\frac{1}{2s} < \omega < \frac{1}{2}$ then the diagonal $x_1 = x_2$ is the unique attractor of (6).

The two types of attractor: \mathcal{D} and the diagonal $x_1 = x_2$, are clearly chaotic and vary continuously with s and ω . Consequently we have the following result.

Corollary 6.2. *Let $\frac{\sqrt{5}+1}{2} < s < 2$. Then (6) has robust chaos for $0 < \omega < \frac{1}{2}$. The attractor is continuous in the Hausdorff metric for $0 < \omega < \frac{1}{2s}$ and $\frac{1}{2s} < \omega < \frac{1}{2}$.*

The region of robust chaos, Fig. 6, is thus divided into two pieces by the curve $\omega = \frac{1}{2s}$ through which the attractor cannot be continued. In this way our consideration of continuity

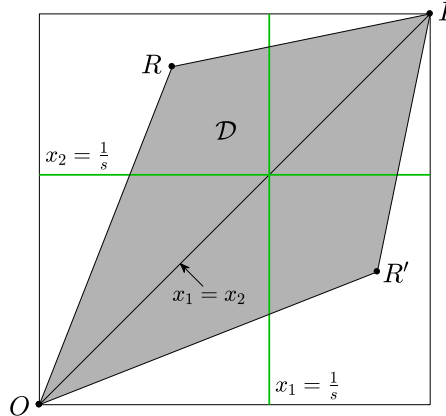


Figure 5: Phase space (x_1, x_2) of the coupled skew tent map (6) showing the quadrilateral \mathcal{D} of Theorem 6.1.

in the Hausdorff metric has allowed us to partition the region of robust chaos into two different types in a formal way.

It could be objected that this example is a boundary case as \mathcal{D} does not satisfy part (iii) of Definition 2.1. In this sense the map has the same status as $x \mapsto 4x(1-x)$ for which the interval $[0, 1]$ is the ‘attractor’ although all points outside this interval diverge. This is a technical nicety that we expect can be circumvented by generalising the skew tent map (5) to

$$\tilde{T}_{s,t}(z) = \begin{cases} sz, & 0 \leq z \leq t, \\ \frac{st}{1-t}(1-z), & t \leq z \leq 1, \end{cases} \quad (7)$$

where $0 < t < \frac{1}{s}$. Numerical experiments suggest that the two-dimensional map obtained by replacing \tilde{T}_s with $\tilde{T}_{s,t}$ in (6) exhibits an analogous continuous quadrilateral attractor that now satisfies part (iii) of Definition 2.1 for some $r > 0$, but it remains to carefully extend the construction of \mathcal{D} given in [15] to allow $t < \frac{1}{s}$.

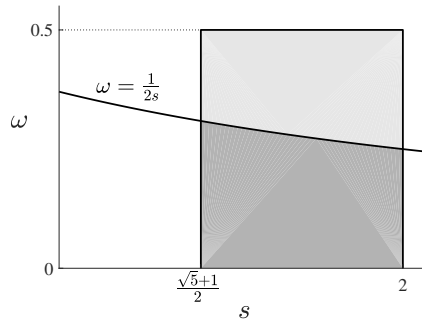


Figure 6: A parameter region of the coupled skew tent map (6) corresponding to robust chaos. Above $\omega = \frac{1}{2s}$ the attractor is the diagonal $x_1 = x_2$; below this curve the attractor is \mathcal{D} , see Fig. 5 and Corollary 6.2.

7 Lozi Maps

The Lozi map [16]

$$L(x) = \begin{bmatrix} 1 - a|x_1| + x_2 \\ bx_1 \end{bmatrix}, \quad (8)$$

where $a, b \in \mathbb{R}$ are parameters, is a piecewise-linear version of the Hénon map. Misiurewicz established robust chaos for (8) in [17].

Theorem 7.1 (Misiurewicz [17]). *Suppose*

$$0 < b < 1, \quad 0 < a < \frac{4-b}{2}, \quad a > \frac{b+2}{\sqrt{2}}, \quad b < \frac{a^2-1}{2a+1}. \quad (9)$$

Then the Lozi map (8) has a unique saddle-type fixed point in $x_1 > 0$ (denoted X) and the closure of the unstable manifold of this point is a chaotic attractor \mathcal{A} .

Here we adapt Misiurewicz's construction to show that the chaotic attractor he obtains varies continuously with a and b . Our proof uses the results of §5 and explains why it was necessary to add the variation of the fundamental converging sets N_μ in that section.

Theorem 7.2. *Throughout the parameter region (9) the attractor \mathcal{A} of Theorem 7.1 is continuous in the Hausdorff metric.*

Proof. Following [17], let X be the fixed point in $x_1 > 0$, let Z be the intersection of the local unstable manifold of X with the x_1 -axis, and let P be the intersection of the local stable manifold of X with the line segment $ZL^2(Z)$, see Fig. 7. Let H_0 be the compact filled triangle XZP . The conditions (9) imply that H_0 is contained in the region $x_1 > 0$, the line segments XZ and ZP belong to the unstable manifold of X , and XP belongs to the local stable manifold of X . It follows that every point on the boundary of the forward invariant set $H = \cup_{k=0}^{\infty} L^k(H_0)$ belongs to either the unstable manifold of X or the line segment XP . Moreover every point on the boundary of $L^n(H)$ belongs to either the unstable manifold of X or the line segment $XL^n(P)$. Notice $d(X, L^n(P)) = \lambda_s^n d(X, P)$, where $0 < \lambda_s < 1$ is the stable eigenvalue associated with X .

Misiurewicz [17] shows that $\cap_{k=0}^{\infty} L^k(H)$ is the attractor \mathcal{A} of Theorem 7.1. By Theorem 5.2 it remains to show that $d_H(L^n(H), \mathcal{A}) \rightarrow 0$ as $n \rightarrow \infty$ uniformly in a and b .

The compact filled triangle $ZL(Z)L^2(Z)$ is forward invariant, see [17], so if K denotes the area of this triangle then $\text{Area}(H) \leq K$. For each n , $\text{Area}(L^n(H)) = b^n \text{Area}(H)$ (because L is invertible and the absolute value of the determinant of the Jacobian matrix of L is b at all points with $x_1 \neq 0$). Thus the distance of any $x \in L^n(H)$ to the boundary of $L^n(H)$ is at most $\sqrt{\frac{K}{\pi}} b^{\frac{n}{2}}$ (obtained by imagining $L^n(H)$ as a circle with centre x and using the Euclidean

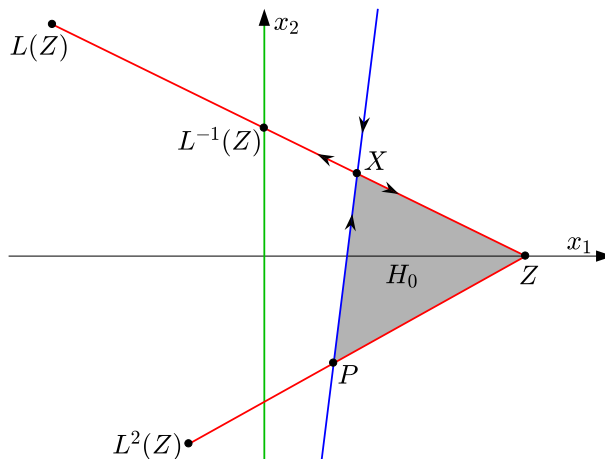


Figure 7: Parts of the stable (blue) and unstable (red) manifolds of the saddle-type fixed point X of the Lozi map (8). Note, the stable eigenvalue associated with X is positive (so the stable manifold has two dynamically independent branches), while the unstable eigenvalue is negative (so the unstable manifold has one dynamically independent branch).

metric). Thus for any $x \in L^n(H)$,

$$d_a(L^n(H), \mathcal{A}) \leq \sqrt{\frac{K}{\pi}} b^{\frac{n}{2}} + \lambda_s^n d(X, P).$$

and since $\mathcal{A} \subseteq L^n(H)$ the same bound applies to $d_H(L^n(H), \mathcal{A})$.

Now fix any pair of parameters $(a_0, b_0) \in \mathbb{R}^2$ satisfying (9). There exists $\delta > 0$ such that (9) is satisfied by all $(a, b) \in \mathbb{R}^2$ a distance at most δ from (a_0, b_0) , call this parameter set M . Denote the supremum values of K , b , λ_s , and $d(X, P)$ over M by K_{\max} , b_{\max} , $\lambda_{s,\max}$, and d_{\max} , respectively. Then for any $(a, b) \in M$ we have

$$d_H(L^n(H), \mathcal{A}) \leq \sqrt{\frac{K_{\max}}{\pi}} b_{\max}^{\frac{n}{2}} + \lambda_{s,\max}^n d_{\max}.$$

Since $b_{\max}, \lambda_{s,\max} < 1$ we conclude that $d_H(L^n(H), \mathcal{A}) \rightarrow 0$ as $n \rightarrow \infty$ uniformly in M_δ . Thus \mathcal{A} is continuous at (a_0, b_0) by Theorem 5.2. \square

8 Border-collision normal form

In this section we describe a numerical example of bifurcations of continuous chaotic attractors in the two-dimensional border-collision normal form

$$x \mapsto \begin{cases} \begin{bmatrix} \tau_L & 1 \\ -\delta_L & 0 \end{bmatrix} x + \begin{bmatrix} 1 \\ 0 \end{bmatrix}, & x_1 \leq 0, \\ \begin{bmatrix} \tau_R & 1 \\ -\delta_R & 0 \end{bmatrix} x + \begin{bmatrix} 1 \\ 0 \end{bmatrix}, & x_1 \geq 0, \end{cases} \quad (10)$$

which has parameters $\tau_L, \delta_L, \tau_R, \delta_R \in \mathbb{R}$. This map, introduced in [18], is a generalisation of the Lozi map and can be used to approximate the dynamics near any generic border-collision bifurcation in two dimensions [19].

We develop an example of [20] and fix

$$\delta_L = 0.3, \quad \delta_R = 0.3. \quad (11)$$

In the (τ_L, τ_R) -plane, see Fig. 8, four codimension-one bifurcation curves, labelled a – d and explained below, divide parameter space into six regions, labelled 1–6. Fig. 9 provides one representative phase portrait for each region. Numerically we observe three continuous chaotic attractors, a three or six-piece attractor \mathcal{A} (purple) in regions 2 and 5, a one-piece attractor \mathcal{B} (yellow) in regions 1–3, and a merging of these two attractors \mathcal{C} (cyan) in region 6.

Let us first describe the four bifurcation curves. Curve a is the locus of a border collision bifurcation. Below curve a there exist unique LRL and RRL -cycles (these are period-3 solutions with the indicated symbolic itineraries [19]). The LRL -cycle is stable in regions 1 and 4. On curve b the LRL -cycle has an eigenvalue of -1 and there exists a period-6 solution with one point on the switching manifold $x_1 = 0$. This solution grows continuously into attractor \mathcal{A} in regions 2 and 5. As τ_L increases, crossing curve b , there is a transition

from the stable LRL -cycle to \mathcal{A} which is not continuous in the Hausdorff metric because the LRL -cycle and period-6 solution do not coincide on curve b . For a greater description of this type of non-smooth period-doubling bifurcation refer to [21, 22]. Curves c and d are the loci of boundary crisis bifurcations which create and destroy the attractor \mathcal{A} (curve c) and \mathcal{B} (curve d). The intersection of these two curves is a codimension two boundary crisis described by [23], and these curves form the boundary of the region in which attractor \mathcal{C} exists.

In all six regions the RRL -cycle is a saddle and its stable and unstable manifolds, W^s and W^u , are shown in Fig. 9. In regions 1 and 2, W^s forms the boundary between the basins of attraction of the two coexisting attractors. The unstable eigenvalue associated with the RRL -cycle is positive so W^u has two dynamically independent branches (and each branch has three pieces).

Points on the ‘outer’ branch of W^u converge (under forward iteration of (10)) to the stable LRL -cycle in regions 1 and 4 and to the attractor \mathcal{A} in regions 2 and 5. The attractor \mathcal{A} is destroyed in a *crisis* on curve c : here the outer branch of W^u attains an intersection with W^s . This is a first homoclinic tangency [24] except W^s and W^u are piecewise-linear so form ‘corner’ intersections [25]. To the right of curve c points on the outer branch converge to the same attractor as points on the inner branch.

In regions 1–3, points on the ‘inner’ branch of W^u converge to the attractor \mathcal{B} . This attractor is destroyed in a crisis on curve d : here the inner branch of W^u attains an intersection with W^s . Below curve d points on the inner branch converge to the same attractor as points on the outer branch.

In region 6 points converge to attractor \mathcal{C} which involves both parts of phase space associated with \mathcal{A} and \mathcal{B} . As we cross curves c or d the transition from \mathcal{A} or \mathcal{B} to \mathcal{C} is not

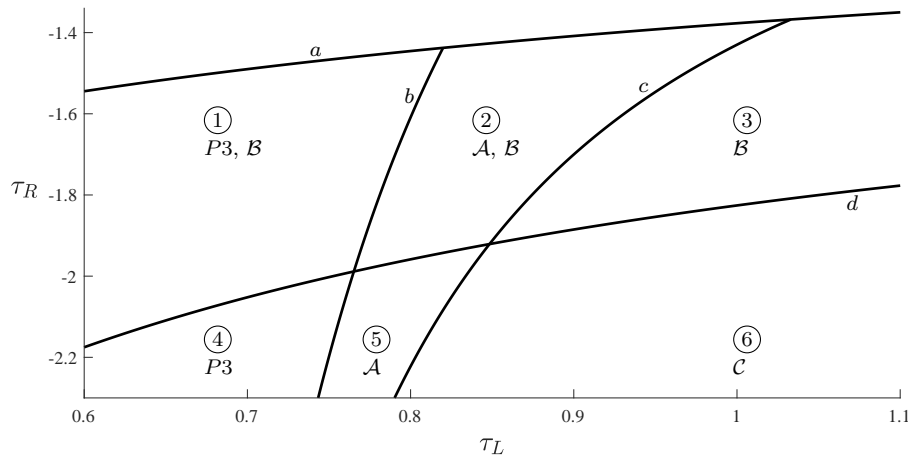


Figure 8: A two-dimensional slice of the parameter space of the two-dimensional border-collision normal form (10) defined by the restriction $\delta_L = \delta_R = 0.3$, (11). The stable period-three orbit (LRL -cycle) is labelled $P3$; the chaotic attractors are labelled \mathcal{A} , \mathcal{B} and \mathcal{C} . The bifurcation curves are a : border collision; b : non-smooth period-doubling; c : boundary crisis of attractor \mathcal{A} ; and d : boundary crisis of attractor \mathcal{B} .

continuous in the Hausdorff metric because the crises cause orbits to suddenly access new areas of phase space.

As an additional visualisation, Fig. 10 shows numerically computed maximal Lyapunov exponents of the attractors. The observation that the Lyapunov exponents of \mathcal{A} , \mathcal{B} , and \mathcal{C} are positive and vary continuously in their respective regions supports our conjecture that these attractors are chaotic and continuous. The Lyapunov exponent varies continuously as we cross from region 6 to region 3 through curve d because as we approach curve d the fraction of iterates of attractor \mathcal{C} that dwell near attractor \mathcal{B} tends to 1 (the invariant measure changes continuously across curve d), and similarly from region 6 to region 5 through curve c .

In summary, (10) has robust chaos in all but region 4 and each chaotic attractor appears to be continuous in the Hausdorff metric in the regions in which it exists. The particular novelty of this example is region 2 where the chaotic attractors \mathcal{A} and \mathcal{B} coexist. One may continue

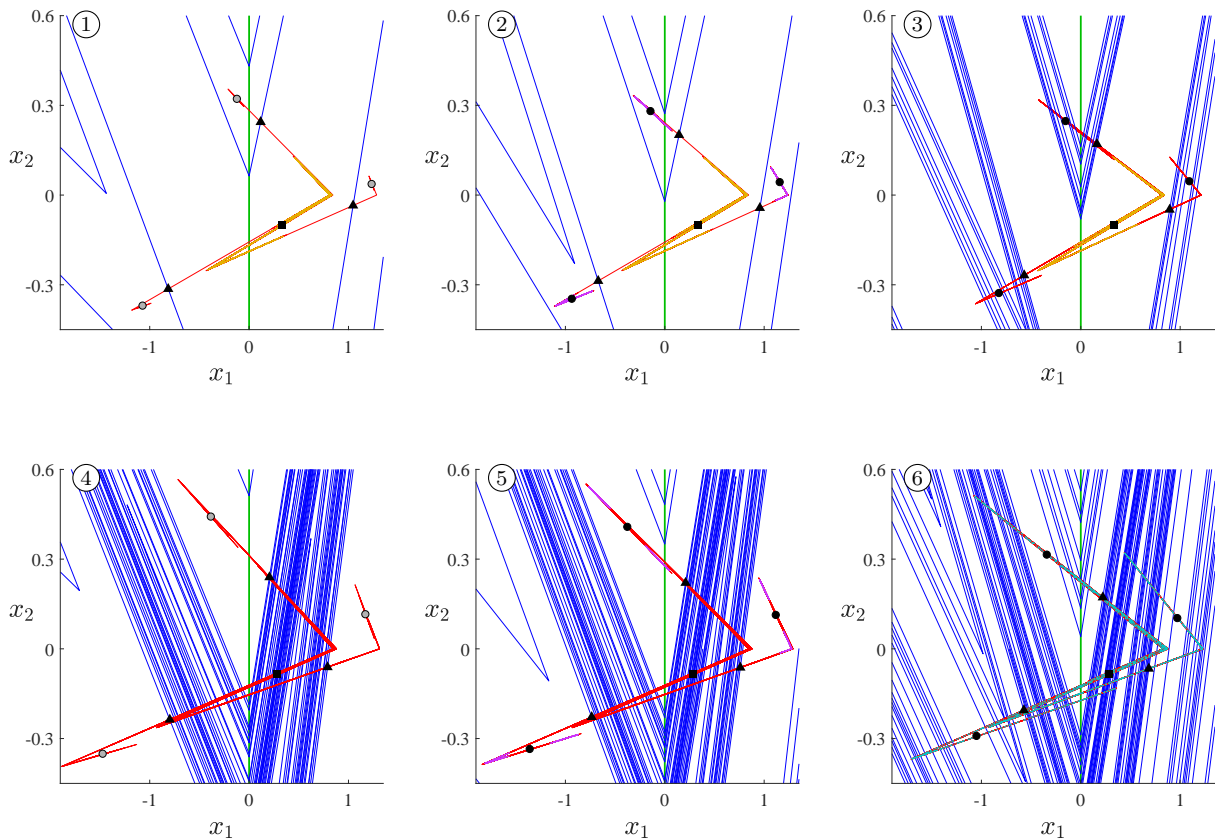


Figure 9: Phase portraits of (10) with (11) for sample parameter values in regions 1–6 of Fig. 8. The fixed point in $x_1 > 0$ is shown with a square, the LRL -cycle is shown with circles, and the RRL -cycle is shown with triangles. The stable and unstable manifolds of the RRL -cycle, W^s and W^u , are shown blue and red respectively (these were computed by numerically growing the manifolds outwards from the RRL -cycle for a large number of iterations). The chaotic attractors \mathcal{A} , \mathcal{B} , and \mathcal{C} are coloured purple, yellow, and cyan respectively.

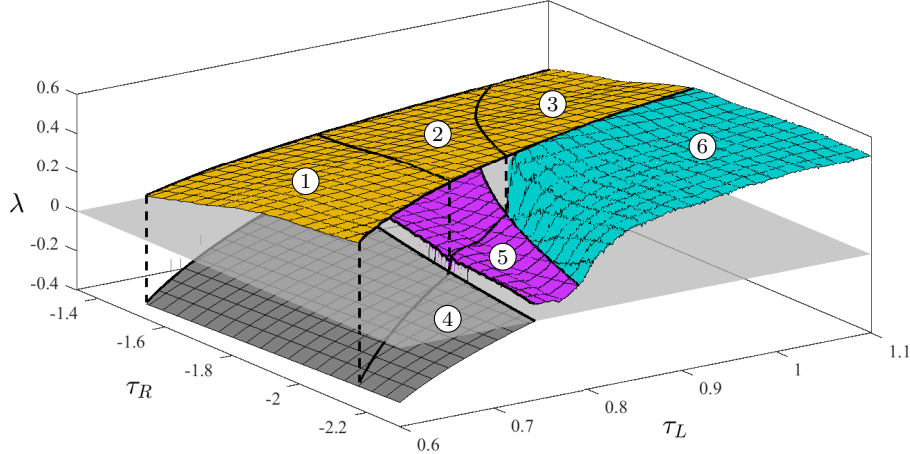


Figure 10: Numerically computed maximal Lyapunov exponents for attractors \mathcal{A} (purple), \mathcal{B} (yellow), \mathcal{C} (cyan), and the LRL -cycle (grey). The bifurcation curves of Fig. 8 have been overlaid for reference. Regions 1 and 2 have coexisting attractors so here there are two surfaces of Lyapunov exponents.

each attractor separately, \mathcal{A} may be continued into region 5, while \mathcal{B} may be continued into regions 1 and 3.

9 Discussion

In this paper we have added depth to the phenomenon of robust chaos in piecewise-smooth maps. Previous works have shown piecewise-smooth maps to exhibit robust chaos in the sense that a chaotic attractor exists throughout an open region of parameter space. In several examples we have found this attractor to be continuous in the Hausdorff metric and in this sense exhibits an extra level of robustness.

In the context of numerical exploration such an attractor could be continued numerically along a one-dimensional path in parameter space. Given attractors at two different points in parameter space, one could ask whether or not there exists a path along which one attractor can be continued into the other. We stress that the continuation of invariant sets and attracting sets is more commonplace. Attractors are more restrictive objects needing, among other things, a dense orbit (see Definition 2.1), and so, as argued in §4, the continuation of a chaotic attractor may only be useful for piecewise-smooth maps.

Rather than use the Hausdorff metric, one could instead consider the continuity of an attractor with respect to its Lyapunov spectrum, the topology of its support (e.g. number of holes), its invariant probability measure [26], or, in the case of piecewise-smooth maps, the fraction of iterates that lie on one side of the switching manifold (which may have a useful physical interpretation). Indeed, as evident from Fig. 10, if one continued attractors using the maximal Lyapunov exponent, attractors \mathcal{A} and \mathcal{B} in region 2 could be connected by a closed path through regions 5, 6, and 3.

References

- [1] S. Banerjee, J.A. Yorke, and C. Grebogi. Robust chaos. *Phys. Rev. Lett.*, 80(14):3049–3052, 1998.
- [2] P. Glendinning. Robust chaos revisited. *Eur. Phys. J. Special Topics*, 226(9):1721–1738, 2017.
- [3] S. van Strien. One-parameter families of smooth interval maps: Density of hyperbolicity and robust chaos. *Proc. Amer. Math. Soc.*, 138(12):4443–4446, 2010.
- [4] P.A. Glendinning and D.J.W. Simpson. Constructing robust chaos: invariant manifolds and expanding cones. *Submitted.*, 2019.
- [5] J.M. Ottino. Mixing, chaotic advection, and turbulence. *Annu. Rev. Fluid Mech.*, 22:207–253, 1990.
- [6] E.M. Bollt and J.D. Meiss. Targeting chaotic orbits to the Moon through recurrence. *Phys. Lett. A*, 204:373–378, 1995.
- [7] L. Kocarev and S. Lian, editors. *Chaos-Based Cryptography. Theory, Algorithms and Applications*. Springer, New York, 2011.
- [8] Stuart. A.M. and A.R. Humphries. *Dynamical Systems and Numerical Analysis*. Cambridge University Press, New York, 1996.
- [9] L. Desheng and P.E. Kloeden. Equi-attraction and the continuous dependence of attractors on parameters. *Glasgow Math. J.*, 46:131–141, 2004.
- [10] L.T. Hoang, E.J. Olson, and J.C. Robinson. On the continuity of global attractors. *Proc. Amer. Math. Soc.*, 143:4389–4395, 2015.
- [11] P. Glendinning. *Stability, Instability and Chaos: An Introduction to the Theory of Nonlinear Differential Equations*. Cambridge University Press, New York, 1994.
- [12] S.J. van Strien. On the bifurcations creating horseshoes. In D.A. Rand and L.-S. Young, editors, *Dynamical Systems and Turbulence, Warwick, 1980*, pages 316–351. Springer, New York, 1981.
- [13] W. de Melo and S. van Strien. *One-Dimensional Dynamics*. Springer-Verlag, New York, 1993.
- [14] A.S. Pikovsky and P. Grassberger. Symmetry breaking bifurcation for coupled chaotic attractors. *J. Phys. A: Math. Gen.*, 24:4587–4597, 1991.
- [15] P. Glendinning. Milnor attractors and topological attractors of a piecewise linear map. *Nonlinearity*, 14(2):239–257, 2001.

- [16] R. Lozi. Un attracteur étrange(?) du type attracteur de Hénon. *J. Phys. (Paris)*, 39(C5):9–10, 1978. In French.
- [17] M. Misiurewicz. Strange attractors for the Lozi mappings. In R.G. Helleman, editor, *Nonlinear dynamics, Annals of the New York Academy of Sciences*, pages 348–358, 1980.
- [18] H.E. Nusse and J.A. Yorke. Border-collision bifurcations including “period two to period three” for piecewise smooth systems. *Phys. D*, 57:39–57, 1992.
- [19] D.J.W. Simpson. Border-collision bifurcations in \mathbb{R}^n . *SIAM Rev.*, 58(2):177–226, 2016.
- [20] V. Avrutin, M. Schanz, and S. Banerjee. Occurrence of multiple attractor bifurcations in the two-dimensional piecewise linear normal form map. *Nonlin. Dyn.*, 67:293–307, 2012.
- [21] D.J.W. Simpson. *Bifurcations in Piecewise-Smooth Continuous Systems.*, volume 70 of *Nonlinear Science*. World Scientific, Singapore, 2010.
- [22] I. Sushko and L. Gardini. Degenerate bifurcations and border collisions in piecewise smooth 1D and 2D maps. *Int. J. Bifurcation Chaos*, 20(7):2045–2070, 2010.
- [23] H.M. Osinga. Boundary crisis bifurcation in two parameters. *J. Diff. Eq. Appl.*, 12(10):997–1008, 2006.
- [24] J. Palis and F. Takens. *Hyperbolicity and sensitive chaotic dynamics at homoclinic bifurcations*. Cambridge University Press, New York, 1993.
- [25] D.J.W. Simpson. Unfolding homoclinic connections formed by corner intersections in piecewise-smooth maps. *Chaos*, 26:073105, 2016.
- [26] J.F. Alves, A. Pumariño, and E. Vigil. Statistical stability for multidimensional piecewise expanding maps. *Proc. Amer. Math. Soc.*, 145(7):3057–3068, 2017.